Global MicroRNA Profiling of HSV-1 Infected Cornea Identifies miR-329 as a Novel Regulator of Virus Infection

Pankaj Sharma,[1] Raza Ali Naqvi,[2] Hemant Borase,[1] Divya Kapoor,[1,3] Araceli Valverde,[2] Kristelle Capistrano,[2] Tejabhiram Yadavalli,[1] Afsar R. Naqvi,[2] and Deepak Shukla[1,3]

[1]Department of Ophthalmology, University of Illinois - Chicago, Chicago, Illinois, United States
[2]Department of Periodontics, College of Dentistry, University of Illinois - Chicago, Chicago, Illinois, United States
[3]Department of Microbiology and Immunology, University of Illinois - Chicago, Chicago, Illinois, United States

Correspondence: Afsar R. Naqvi, Department of Periodontics, College of Dentistry, University of Illinois - Chicago, 801 S. Paulina Street, Room 458, MC 859, Chicago, IL 60612, USA; afsarraz@uic.edu.
Deepak Shukla, Department of Ophthalmology, University of Illinois - Chicago, 1855 W Taylor Street, Chicago, IL 60612, USA; dshukla@uic.edu.

PS and RAN contributed equally to this study.

Received: January 3, 2025
Accepted: February 2, 2025
Published: February 24, 2025

Citation: Sharma P, Naqvi RA, Borase H, et al. Global MicroRNA profiling of HSV-1 infected cornea identifies miR-329 as a novel regulator of virus infection. *Invest Ophthalmol Vis Sci.* 2025;66(2):61. https://doi.org/10.1167/iovs.66.2.61

Purpose. Although the mechanisms underlying herpes simplex virus type-1 (HSV-1) ocular infection have been extensively studied, the role of host microRNAs (miRNAs) in the pathobiology of herpetic keratitis (HK) is not well understood. The aim of this study was to identify endogenous miRNA regulators involved in the progression of HSV-1 ocular infection.

Methods. C57BL/6 mice were infected with HSV-1 strain McKrae following epithelial debridement, and corneal miRNA profiles were analyzed at various time points using miRNA sequencing (miRNA-seq). The miRNA expression was measured at 2, 4, 6, and 10 days post-infection. Ingenuity Pathway Analysis (IPA) was used to identify immune pathways potentially targeted by differentially expressed miRNAs. The role of selected miRNAs in viral entry and replication was assessed by overexpression in murine embryonic fibroblasts (MEFs) and human corneal epithelial cells (HCEs).

Results. A total of 32 miRNAs at 2 days post-infection, 21 miRNAs at 4 days post-infection, 140 miRNAs at 6 days post-infection, and 27 miRNAs at 10 days post-infection showed significant changes in expression. IPA revealed that differentially expressed miRNAs targeted several immune pathways, including TLR and interferon signaling. Notably, mmu-miR-184-3p and mmu-let-7d-5p were upregulated, whereas mmu-miR-329-3p was down-regulated during infection. Functional assays demonstrated that overexpression of miR-329, but not miR-184-3p or miR-let-7d-5p, increased HSV-1 viral entry and replication in a dose-dependent manner. In contrast, miR-329 inhibition reversed these effects, suggesting its role as a pro-viral miRNA. Increased plaque formation and viral gB expression further confirmed miR-329's pro-viral role.

Conclusions. Our findings suggest that miR-329 functions as a pro-viral miRNA by disrupting TLR9 signaling, thus facilitating HSV-1 replication. Inhibition of miR-329 enhances TLR9-mediated antiviral responses, highlighting the potential of targeting host miRNAs as a novel therapeutic strategy for managing viral keratitis.

Keywords: herpes simplex virus type-1 (HSV-1), microRNAs (miRNAs), herpes keratitis (HK), antiviral immunity, viral replication

Herpes simplex virus type 1 (HSV-1) infection poses an unembellished threat to ocular health. Alarmingly, approximately 50,000 new cases of ocular herpes occur every year in the United States.[1] Blepharitis, follicular conjunctivitis, keratitis, and keratouveitis are some frequent manifestations of ocular HSV. After primary infection, HSV-1 moves to the trigeminal ganglion (TG) and becomes latent.[2] Whereas many host factors that modulate HSV-1 infection of the eye have been identified,[3–8] there is limited knowledge regarding the role of non-protein factors, such as micro RNAs (miRNAs), in ocular infection. Identifying the miRNAs that regulate primary infection in the cornea is crucial for developing a comprehensive understanding of herpetic tissue tropism and for developing novel therapeutic targets to mitigate the clinical manifestations of viral keratitis. Although growing evidence suggests that herpesviruses exploit the dysregulation of host miRNAs to create favorable conditions for replication or latency,[9–11] the specific role of corneal tissue-expressed miRNAs in HSV-1 infection remains poorly understood. As defined previously, miRNA is a class of small non-coding RNA that post-transcriptionally regulate essentially every cellular activity by binding to cognate transcripts harboring complementary sequences.[12] The miRNAs are transcribed as pri-miRNAs (precursor transcript), which has the tendency to form a typical hairpin structure. Through a series of RNA endonucleases, this precursor is processed to generate a single stranded RNA that guides a protein complex, called miRNA-induced silencing complex (miRISC) containing Argonaute (Ago).[13] Upon miRNA binding to a cognate transcript, RISC activity either promotes target transcript degradation or translational repression affecting translational output.[14] During viral infections miRNAs are

emerging as the key regulators of host-virus interaction by shaping pathways involved in antiviral immunity or viral life-cycle. The first host miRNA demonstrated to affect the replication of hepatitis C virus (HCV) was recognized as liver specific miR-122, which binds to 5′UTR of HCV genome at a point upstream to internal ribosome entry site (IRES) and increases virus production.[4,5] Binding of Ago proteins to 5′UTR of HCV genome stabilizes the RNA genome by inhibiting its decay.[10,15] Conversely, Heiss et al. demonstrated that introducing the cognate sequence of miR-9, miR-124, or let-7c into the genome of neurotropic chimeric tick-borne encephalitis virus/dengue virus 4 (TBEV/DEN4) flavivirus prevents the development of encephalitis in adult mice.[16] Therefore, miRNA targeting can be used as good strategy for controlling the virus tropism. Furthermore, miR-142-3p effectively restrains the mosquito-borne North American eastern equine encephalitis virus (EEEV) replication in myeloid-lineage cells via targeting its genome.[17] Similarly, miR-27 exhibited a potent antiviral function for murine cytomegalovirus (MCMV).[18,19] In the context of HSV-1, Pan et al. showed that the host miR-138 targets the HSV-1 derived ICP0, a key viral protein involved in the reactivation, and therefore promotes the establishment of latency.[20] Besides viral tropism, cellular miRNAs are key regulators of antiviral immunity. For instance, HSV-1 induced miR-23a in HeLa cells target interferon regulatory transcription factor 1 (IRF1)[21–23] and facilitate the viral infection. On the contrary, overexpression of miR-32a inhibits the replication of Porcine reproductive and respiratory syndrome virus (PRRSV) via induction of IFN response.[24] Interestingly, HSV-1 mediated induction of Behcet's disease in mice also induces miR-21, which ameliorate the suppression of apoptosis in infected cells.[25] These observations highlight a central role of cellular miRNAs in controlling viral tropism and immunity. However, the role of cellular miRNAs in corneal HSV-1 infection remains understudied.

In this study, we evaluated the time kinetics of cellular miRNAs expression in HSV-1 infected mice corneas. We characterized the role of the three most significantly dysregulated miRNA on HSV-1 tropism entry, and replication, in mouse embryonic fibroblasts (MEFs) and human corneal epithelial cells. Among these miRNAs, overexpression of miR-329 promotes viral entry, replication, and formation of infective virions. Mechanistically, miR-329 targets viral recognition and immune signaling that are critical in mounting a robust antiviral state. Our results show a novel role of miR-329 as a potential cellular pro-viral factor, which is downregulated during HSV-1 infection and offers potential avenues for therapeutic intervention.

Methods

Cells and Viruses

Human corneal epithelial cells (HCE-T and RCB1834) were generously provided by Kozaburo Hayashi (National Eye Institute, Bethesda, MD, USA). These cells were maintained in Minimum Essential Medium (MEM; Life Technologies, Carlsbad, CA, USA) supplemented with 10% fetal bovine serum (FBS; Sigma-Aldrich, St. Louis, MO, USA) and 1% penicillin-streptomycin (P/S; Life Technologies, Carlsbad, CA, USA). African green monkey kidney (Vero) cells, along with HSV-1 17-GFP and McKrae strains, were obtained from Homayon Ghiasi (Cedars Sinai Health System, Los Angeles, CA, USA) and cultured in Dulbecco's Modified Eagle's Medium (DMEM; Life Technologies, Carlsbad, CA, USA) supplemented with 10% FBS and 1% P/S. All cells were maintained under standard conditions in a Heracell VIOS 160i CO_2 incubator (Thermo Fisher Scientific, Pittsburgh, PA, USA). MEFs were kindly provided by Dr. Israel Vlodavsky (Rappaport Institute).

Mice Ocular Infection

This study was approved by the University of Illinois Chicago Animal Care Committee and adhered to the ARVO Statement for the Use of Animals in Ophthalmic and Vision Research. Male C57BL/6 mice (6–8 weeks old, $n = 25$) were obtained from Charles River Laboratories (Wilmington, MA, USA) and housed at the Biologic Resources Laboratory (BRL), University of Illinois - Chicago. The mice were anesthetized with ketamine (100 mg/kg) and xylazine (5 mg/kg), followed by application of proparacaine hydrochloride (Alcon Laboratories, Fort Worth, TX, USA) to the right eye to numb the area before scarification. Anesthesia efficacy was confirmed by the loss of pedal reflex.

The corneal epithelium of the right eye was debrided with a 30 G sterile needle in a 3 × 3 grid pattern, and each eye was infected with 1×10^5 PFU/mL of HSV-1 strain McKrae. Mock-infected mice received Vero cell lysate. The mice were euthanized on days 2, 4, 6, and 10 post-infection ($n = 5$/group), and total RNA was extracted from the eyes. All procedures were conducted in a BSL2 rodent facility.

Small RNA Library Construction and Sequencing

Total RNA was extracted from murine corneas using the miRNeasy Kit (Qiagen, Valencia, CA, USA) as per the manufacturer's instructions. RNA quality and quantity were assessed using the Bioanalyzer 2100 with the RNA 6000 Nano LabChip Kit (Agilent, Santa Clara, CA, USA). Approximately 1 µg of RNA was used to construct small RNA libraries with the TruSeq Small RNA Sample Prep Kit (Illumina, San Diego, CA, USA). Libraries were sequenced as single-end reads (50 bp) on an Illumina HiSeq 4000 at LC Sciences.

Bioinformatics Analysis

Raw sequencing reads were processed using ACGT101-miR (LC Sciences, Houston, TX, USA) to eliminate adapter dimers, junk sequences, low complexity regions, common RNA families (rRNA, tRNA, snRNA, and snoRNA), and repetitive elements. Unique sequences ranging from 18 to 26 nucleotides were then aligned to species-specific precursors in miRBase 21.0 using BLAST to identify both known miRNAs and novel 3p- and 5p-derived variants. The alignment parameters allowed for length variations at both the 3' and 5' termini and permitted one internal mismatch. Sequences aligning to known mature miRNAs within hairpin arms were classified as known miRNAs. Sequences mapping to the opposite arm of known precursor hairpins, relative to the annotated mature miRNA arm, were designated as novel 5p- or 3p-derived miRNA candidates. Additional sequences were mapped to precursors from other selected species in miRBase 21.0 (excluding the specific species of interest), followed by BLAST analysis against the specific species genome to determine genomic locations. These two categories were classified as known miRNAs. The remaining unmapped sequences underwent BLAST analysis against specific genomes, and potential hairpin RNA structures were

predicted using RNAfold software by analyzing 80 nt flanking sequences. The structural prediction criteria included maximum stem bulge size of 12 nucleotides, minimum 16 base pairs in stem region, maximum free energy of −15 kCal/mol, minimum total hairpin length of 50 nucleotides (including stems and terminal loop), maximum loop length of 20 nucleotides, maximum 8 nucleotides per bulge in mature region, maximum 4 biased errors per bulge in mature region, maximum 2 biased bulges in mature region, maximum 7 total errors in mature region, minimum 12 base pairs in mature region, and minimum 80% mature sequence presence in the stem.

Overview of Reads From Raw Data to Clean Data

Raw sequencing data were processed using the ACGT101-miR filter module to remove low-quality reads, 3′ adapter sequences, and contaminants. Clean sequences (≥18 nt) were annotated in the Rfam database (http://www.sanger.ac.uk/software/Rfam) to exclude non-coding RNAs (rRNA, tRNA, snRNA, and snoRNA) and mRNA degradation fragments. Remaining sequences were aligned to the miRBase database (release 21) (http://www.miRbase.org/), and perfectly matched sequences were identified as conserved *Mus musculus* miRNAs.

Identification of Conserved and Novel miRNAs

Unique reads processed through the ACGT101-miR filter module were analyzed to identify conserved and novel *Mus musculus* miRNAs. The reads were mapped to miRNAs and pre-miRNAs in miRBase, with pre-miRNAs further aligned to the genome and EST in various categories. In gp1a, reads mapped to species-specific miRNAs/pre-miRNAs and were further aligned to the genome and EST. Similarly, in gp1b, reads aligned to miRNAs/pre-miRNAs of selected species and the genome. In gp2a, reads mapped to pre-miRNAs not aligned to the genome but matched extended genome sequences capable of forming hairpins, whereas in gp2b, reads mapped to pre-miRNAs not aligned to the genome, and the extended sequences failed to form hairpins. In gp3, reads aligned to mature miRNAs without mapping to pre-miRNAs or the genome, and, in gp4, reads did not align to pre-miRNAs but matched genome sequences capable of forming hairpins.

Sequence counts were normalized by dividing the counts by a library size parameter, determined as the median ratio of counts between a sample and a pseudo-reference sample, where the pseudo-reference sample counts represented the geometric mean across all samples. Differential expression analysis was performed using Fisher's exact test, Chi-squared tests (2 × 2 or nXn), Student's *t*-test, or ANOVA based on the experimental design. Statistical significance was determined with thresholds set at $P < 0.01$ or $P < 0.05$.

IPA and miRNA Target Prediction

To investigate the role of differentially expressed miRNAs in the murine cornea, web-based Ingenuity Pathway Analysis (IPA) was performed. Gene targets of the most abundant miRNAs were predicted using two computational algorithms, TargetScan (http://www.targetscan.org/) and Miranda 3.3a (http://www.microrna.org/), to identify miRNA binding sites. The predictions from both algorithms were combined, and overlaps were calculated. The miRNA-mRNA interactions were further analyzed using the miRNA target filter and canonical pathway features of IPA (QIAGEN 2013–2023). IPA integrates data from miRBase, TargetScan, and the QIAGEN Knowledge Base to provide insights into biological functions, canonical pathways, and networks. Differentially expressed miRNAs were uploaded to IPA and filtered by confidence level (moderate, high, or experimentally validated) and pathways (TLR and interferon). Figures were generated using IPA's Path Designer for graphical representation.

Transfection of miRNA Mimics or Inhibitors

Synthetic LNA mimics and inhibitors of miR-329, miR-184, and let-7d were procured from Thermo Fisher Scientific, USA. RNA oligos were transfected (at a final concentration of 25 nM and 50 nM) in human corneal epithelial (HCE) cells and MEFs using Lipofectamine 2000 (Invitrogen, Carlsbad, CA, USA), as per the manufacturer's instructions.

Flow Cytometry

The replication of HSV-1 17-GFP was assessed by flow cytometry. After 24 hours post-infection, the wells were washed twice with PBS and then treated with trypsin. The cells were then treated with complete media (DMEM, 10% FBS, and 1% Pen-Strep) to inactivate trypsin, washed two times in PBS-BSA (1%), and resuspended in the same buffer. The single cell suspension was then subjected to flow cytometry analysis for GFP expression as a reflection of HSV-1 infection on Accuri C6 flow cytometer (BD Sciences). An equal number of events (20,000) were captured for all the samples. The doublets were excluded from the analysis based on FSC-A versus FSC-H. Flow cytometry data was quantitated on FlowJo version 10.9.0.

Fluorescence Microscopy

Lionheart LX (BioTek) automated imaging system was used to acquire the images of HSV-1 17-GFP infected cells. As per the instructions of this imaging system, multiple images of HSV-1 infected cells were taken together, which were automatically stitched by the BioTeK software.

Western Blotting

Cells were collected in Hank's buffer (Gibco), centrifuged at 800 × g for 10 minutes, and the supernatant was discarded. RIPA buffer was added to the pellet, and the samples were incubated on ice for 30 minutes, followed by centrifugation at 12,000 × g for 30 minutes at 4°C. The viral lysate was mixed with NuPAGE LDS Sample Buffer (Invitrogen, NP00007) and heated at 80°C for 10 minutes. Equal amounts of protein were loaded onto a 4% to 12% SDS-PAGE gel, and the proteins were transferred to a nitrocellulose membrane using an Invitrogen iBlot2 fast-dry transfer system. After transfer, the membrane was blocked in 5% nonfat milk in 1 × Tris-buffered saline (TBS) for 2 hours at room temperature to prevent nonspecific antibody binding. The membrane was then incubated overnight at 4°C with primary antibodies, including TNFAIP3 (Proteintech, 66695-1-Ig), MYD88 (Proteintech, 67969-1-Ig), IRAK4 (Proteintech, 18221-1-AP), REL (Proteintech, 67747-1-Ig), IKBKG (Proteintech, 18474-1-AP), IRF3 (Proteintech, 11312-1-AP), Phospho-IRF3 (Proteintech, 29528-1-AP), IRF7 (Protein-

Investigative Ophthalmology & Visual Science

tech, 22392-1-AP), β-Actin (Proteintech, 20536-1-AP), TLR9 (AbClonal, A14642), Anti-HSV1+HSV2 gB (Abcam, 10B7), Anti-HSV1+HSV2 VP16 (Abcam, ab110226), and Phospho-IRF7 (Cell Signaling, D7E1W). After washing 3 times with 0.1% TBS, the membrane was incubated with HRP-conjugated anti-mouse IgG (1:25,000) at room temperature.

Plaque Assay

Whole cell lysates (from both HCEs and MEFs) and culture supernatants from HSV-1-infected cells were used for plaque assays. After 24 hours of infection, the cells were collected in Hank's cell dissociation buffer (Gibco), washed with 1 × PBS, and resuspended in 1 mL OptiMEM (Gibco). The resuspended cells were sonicated using a probe sonication system (5-second pulses at 20% amplitude for up to 30 seconds). Both the cell lysates and culture supernatants were serially diluted to a final dilution of 10^{-8} in 1 mL. Vero cell monolayers were overlaid with 250 µL of each dilution (4-fold dilution in a 24-well plate). After 2 hours, the cells were washed with PBS and overlaid with 5% methylcellulose (Sigma-Aldrich) in DMEM, and then incubated at 37°C (5% CO2) for 72 hours until the plaques appeared. Cells were fixed with 250 µL of 100% methanol for 10 minutes and stained with 250 µL crystal violet solution for 30 minutes. Plaques were counted manually after aspirating the solution, and the plaque-forming units per mL (PFU/mL) were calculated by multiplying the plaque count by the appropriate dilution factor.

Viral β-Galactosidase Entry Assay

Previously established protocol was used to evaluate the viral entry. Approximately, 2×10^4 cells per well in a 96-well plate were seeded. Cells transfected with miRNA mimics and their corresponding inhibitors separately were inoculated with recombinant HSV-1 strain gL86 (a portion of the gL gene is replaced with the lacZ gene encoding β-galactosidase), which can only be expressed by the cells after successful viral entry. After 6 hours post-infection, the cells were washed with PBS and were incubated at 37°C for 1 hour with ONPG solution (Thermo Fisher Scientific; 3 mg/mL + 0.05% NP-40) and the colorimetric substrate was detected at 410 nm using a microplate reader.

Statistical Analysis

The statistical analyses were performed using GraphPad Prism version 10. One way ANOVA was conducted to calculate the significance. All the experiments were performed in triplicate. $^{*}P < 0.05$; $^{**}P < 0.01$; $^{***}P < 0.001$; and $^{****}P < 0.0001$.

Results

HSV-1 Infection in Corneal Tissue Alters MicroRNA Profiles

The miRNAs demonstrate tissue-specific expression and vary in expression levels under different physiological and pathological circumstances.[26,27] To elucidate the dynamics of miRNA expression alterations during ocular infection HSV-1, we conducted kinetics of miRNA profiles in mice infected with HSV-1 McKrae. Samples were collected at 2, 4, 6, and 10 days post-infection and compared against mock-infected controls ($n = 4$/group). Figure 1A depicts the schematic of the mice infection experiment. A total of 13.96 ± 5.8 million (Mock), 21.6 ± 7.8 million (2 days post-infection), 13.3 ± 2.5 million (4 days post-infection), 10.6 ± 3.2 million (6 days post-infection), and 11.2 ± 1.3 million (10 days post-infection) raw reads were obtained by miRNA-seq (Supplementary Table S1). After quality control and genome mapping, approximately, 3.4, 4.3, 3.1, 3.3 and 3.2 million of reads were obtained for mock, 2 days post-infection, 4 days post-infection, 6 days post-infection and 10 days post-infection, respectively (Supplementary Table S1).

Our analysis revealed time-dependent changes in the global miRNA profiles throughout HSV-1 infection. Applying fold change thresholds between –1.25 and 1.25 and significance criteria of $P < 0.05$, we identified the following numbers of differentially expressed miRNAs: 32 miRNAs at day 2 (5 downregulated and 27 upregulated), 21 miRNAs at day 4 (13 downregulated and 8 upregulated), 140 miRNAs at day 6 (76 downregulated and 64 upregulated), and 27 miRNAs at day 10 (15 upregulated and 11 downregulated; Fig. 1B). Notably, we observed a peak in the number of differentially expressed miRNAs at day 6. The list of differentially expressed miRNAs at each time point is provided in Supplementary Tables S1 to S4. The heatmaps display the distinct expression patterns of up- and downregulated miRNAs across different time points in HSV-1-infected mice compared to mock-infected counterparts (Fig, 1C, see Supplementary Tables S1–S4).

To discern the distinctive and common subsets of differentially expressed miRNAs during HSV-1 infection, we compared miRNA profiles at each time point. Utilizing a 4-set Flower Venn diagram, we observed a total of 24, 7, 127, and 12 miRNAs specifically expressed in the infected cornea at days 2, 4, 6, and 10, respectively (Fig. 1D). These results show that a large proportion of dysregulated miRNAs are unique to each time point indicating time-dependent changes in corneal miRNA profiles.

We selected miR-329-3p, miR-184-3p, and let7d-5p for further functional assessment because they were significantly dysregulated compared to mock, showed progressive changes during the course of infection, and exhibit 100% sequence conservation between the mouse and a human. Interestingly, these miRNAs showed unique time-dependent induction in their expression cornea infection. The miR-329-3p expression increased at 2 days post-infection but significantly reduced from 4 days post-infection compared to mock. Expression of let7d-5p showed increase at day 6 (approximately 4-fold) and then maintained as an upregulation at a later time point. However, mmu-miR-184 was selectively upregulated at day 6 (approximately 10-fold) and could not be detected at other time points (days 2, 4, and 10; Figs. 1E–G). Overall, these findings suggest that the acquisition of a distinct miRNA repertoire may potentially play a regulatory role in HSV-1 infection of ocular tissues.

Differentially Expressed miRNAs Target Key Pathogen Recognition and Antiviral Signaling Pathways

To identify the global biological impact of HSV-1 infection responsive miRNAs, we used IPA to identify the targets of significantly up- and downregulated miRNAs. Our

Investigative Ophthalmology & Visual Science

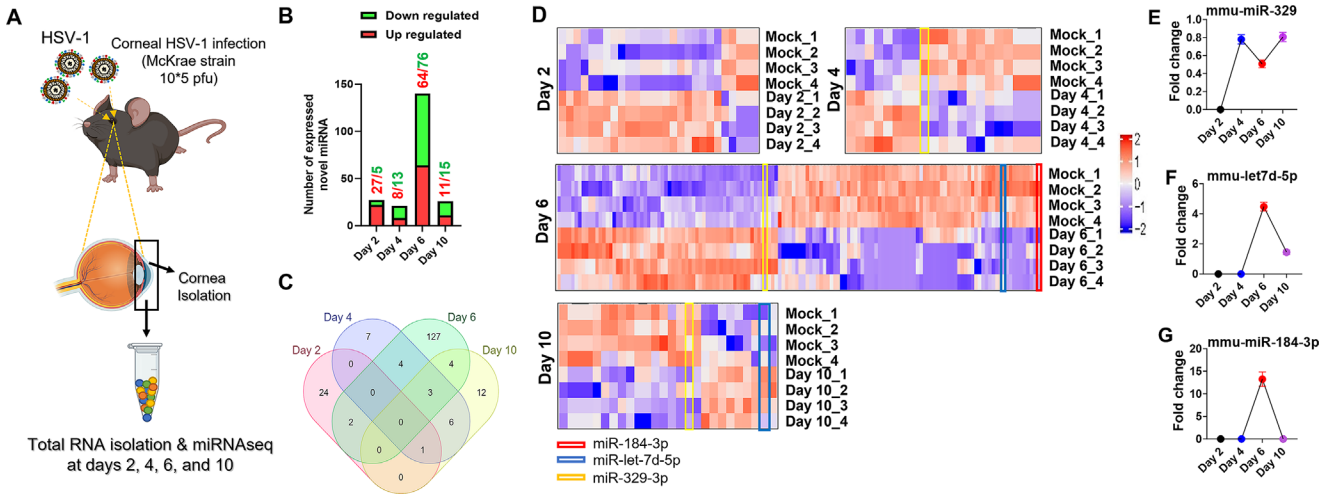

Figure 1. HSV1 infection temporally alters host miRNA expression in mice cornea. (**A**) Schematic showing experimental design for HSV-1 infection in mice cornea. (**B**) Mice were infected with HSV-1 (McKrae strain) and the cornea was collected at different time points of infection ($n = 4$ mice/group). Total cellular RNA isolated from infected cornea was profiled for miRNA expression using miRNA sequencing. Differentially up- and downregulated miRNAs from mice cornea at different time points of HSV-1 infection: day 2, day 4, day 6, and day 10. A cutoff value between –1.25 and 1.25 and $P < 0.05$ (multiple ANOVA) was set to identify differentially expressed miRNAs. (**C**) Heatmaps depicting the expression pattern of significantly altered miRNAs in HSV1-infected cornea compared to mock. (**D**) Venn diagram showing the number of unique and common miRNAs expressed at different time points post-HSV-1 infection. Expressional patterns of selected miRNA (**E**) mmu-miR-329-3p, (**F**) mmu-let7d-5p, and (**G**) mmu-miR-184-3p at various time points of mice cornea infection. In (**E**, **F**) all the bars are generated in GraphPad Prism 10 with the mean values of fold change with respect to mock infected mice cornea. These data are obtained from 4 mice from each group: mock, day 2, day 4, day 6, and day 10 of post HSV-1 infection.

results reveal a dramatic increase in the number of target genes on the later time points, particularly days 4 and 6 post-HSV-1 infection, compared to day 2 or day 10 post-infection in the HSV-1 infected cornea, mmu-miR-184-3p and mmu-let-7d-5p were among the abundant and upregulated miRNAs, whereas mmu-miR-329-3p and mmu-miR-2478 were significantly downregulated. Because miRNAs are canonically negative regulators of gene expression,[28,29] after miRNA sequencing, we interrogated the mRNA targets of the most abundantly upregulated miRNAs at later time points of day 6 and day 10 of HSV-1 infection: mmu-miR-184-3p and mmu-let-7d-5p. Specifically, we focused on the genes involved in Toll-like receptor (TLR) and interferon signaling, essential in orchestrating the immune response to HSV-1 infections. IPA identified imperative target genes for these miRNAs in TLR pathway and IFN signaling (Fig. 2A). In the TLR pathway: (1) mmu-let-7d-5p notably targets TLR4 and its downstream signaling molecules TOLLIP, TAB2, CHUK, MAP3K1, MAP4K4, MAPK11, IL1, and IL12; (2) mmu-miR-184-3p notably targets IKBKB and TOLLIP, which are also downstream of TLR4; and (3) mmu-329-3p targets IKBKG, IRAK4, MYD88, REL, TLR9, and TNFAIP3 genes (see Fig. 2). Moreover, TLR4 signaling activates type I interferons (IFN-α and IFN-β),[30] crucial in limiting viral replication and promoting the antiviral response.[31] In turn, IFN-α and IFN-β upregulate interferon-stimulated genes' expression, inhibiting viral replication and blocking viral spread (Takaoka, 2021). Our IPA analysis reveals that IFNAR1, STAT2, and TYK2 are putative targets of let-7d-5p indicating its potential role in host-virus interaction (Fig. 2B). However, significantly downregulated miR-329 also demonstrated following predicted target in TLR pathways: IKBKG, IRAK4, MYD88, REL, TLR9, and TNFAIP3. Furthermore, OAS1 found to be the target of miR-329 among interferon signaling mRNAs indicating its role as a negative regulator of antiviral activity. Our pathway's analysis suggest that HSV-1 infection may impair numerous biological pathways by dysregulating host miRNAs via modulating the key players of virus recognition (TLR pathways) and antiviral interferon pathways.

HSV-1-Responsive Host miRNAs Regulate Viral Entry and Replication

The miRNA regulates a multitude of cell biological processes, which may play a critical role in host-virus interaction. Our data show that HSV-1 infection alters the corneal miRNA profile, and differentially expressed miRNAs may be key determinants of virus infection in host cells. Viral entry is the first step in the viral infection in this context, which involves attachment of viral proteins to the specific receptors, fusion with host cell membranes in case of enveloped viruses, and finally the delivery of viral genome inside the cells.[32,33] In case of HSV-1 infection, miRNA regulating this rate limiting step remains elusive.

Contemplating it, we asked whether the overexpression or inhibition of candidate dysregulated miRNAs (miR-329, miR-184, and let-7d) may impact HSV-1 entry. Due to 100% sequence homology between murine and human miR-329, miR-184-3p, and let-7d miRNAs, we were able to examine their biological function in both murine and human cells. We transfected mouse embryonic fibroblasts with various concentrations (25 and 50 nM) of miR-329-3p, miR-184-3p, and let-7d-5p, or scramble mimic or inhibitors and infected the cells with HSV-1 gL86 to assess viral entry using a colorimetric assay. Compared to scramble mimic, miR-329-3p overexpression markedly increased (OD values 0.15 ± 0.01 [25 nM] and 0.19 ± 0.003 [50 nM] compared to control mimic 0.13 ± 0.008 [25 nM] and 0.133 ± 0.01 [50 nM]) the entry

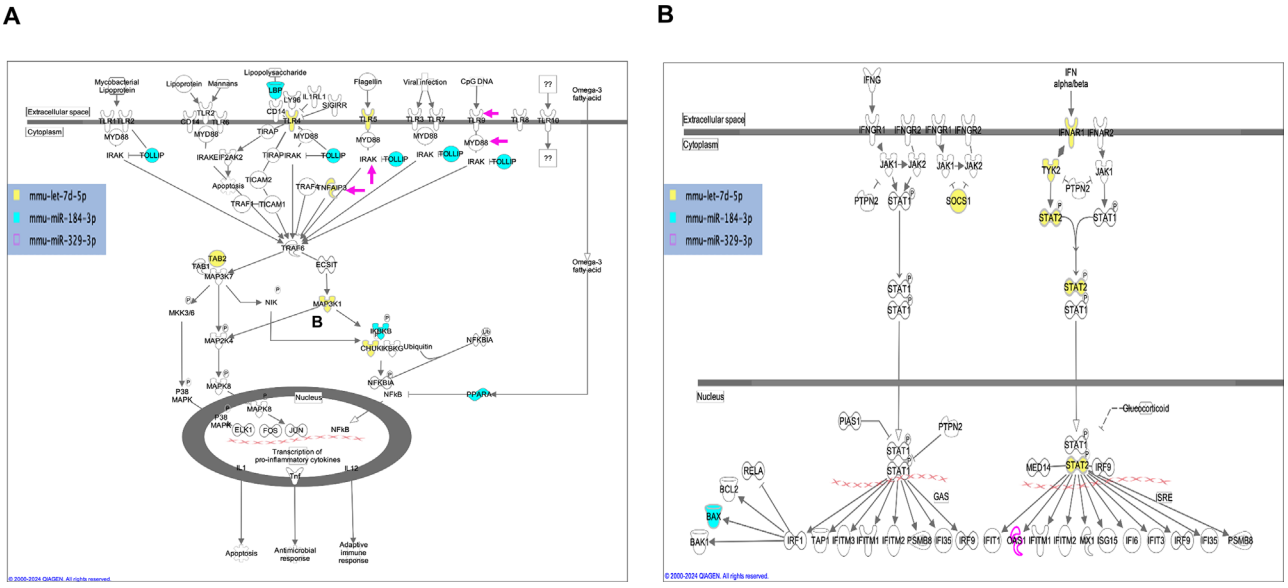

Figure 2. Predicted targets of host miRNA responsive to HSV-1 infection. (**A**) Targets of mice miRNAs miR-184-3p, let7d-5p, and miR-329 in toll-like receptor pathway. (**B**) Targets of the said miRNAs in anti-viral interferon pathway. All these targets were identified through IPA's miRNA Target Filter Analysis. These potential mRNA targets are moderately predicted, or highly predicted or experimentally validated. Target genes are highlighted in various colors specific to miRNA.

of HSV-1 in a dose-dependent manner (Fig. 3A). Conversely, mmu-miR-329-3p inhibitor reduced (0.11 ± 0.01 and 0.08 ± 0.007, respectively, for 25 nM and 50 nM concentrations) the viral entry compared to the control inhibitor at both concentrations (0.13 ± 0.01 and 0.13 ± 0.008) suggesting a role of miR-329 in HSV-1 tropism. These data reflect significantly higher viral entry in miR-329 overexpressing cells. On the contrary, mmu-miR-184-3p mimic and let7d-5p mimic exhibit no biological impact on HSV-1 entry (see Fig. 3A). Together, these results suggest that overexpression of miR-329 promotes the HSV-1 entry. We further validated the impact of candidate miRNAs in HCEs and observed similar results with miR-329 mimic and inhibitor showing higher and reduced viral entry respectively (Supplementary Figs. S1A, S1B).

Next, to address the effect of the above host miRNAs on the replication of HSV-1, we infected the miRNA mimic or inhibitor transfected MEF and HCE with GFP expressing virus HSV-1 17 GFP. Our flow cytometry data show that compared with control mimic, overexpression of miR-329 significantly promoted the HSV-1 17 GFP replication in MEFs in a dose-dependent manner (Fig. 3C). Supplementary Figure S2 is showing the gating strategy to evaluate GFP+ cells. The percentage of GFP+ cells, indicative of viral replication, in miR-329 mimic transfected cells were significantly higher compared with the control mimics. MEFs transfected with miR-329 mimic show 24.62 ± 3.32% (25 nM) and 30.09 ± 1.48% (50 nM) GFP+ cells compared to control mimic 18.9 ± 1.1% (25 nM) and 20.36 ± 1.04% (50 nM). Conversely, inhibition of miR-329-3p reduced viral replication further supporting its role in pro-viral function. The transfection of MEFs with miR-329-3p inhibitors showed significantly less GFP+ cells 15.86 ± 1.71% (25 nM) and 15.15 ± 1.57% (50 nM). The percentages of GFP+ cells did not show a significant change in either miR-184-3p (for mimic = 18.16 ± 3.15% [25 nM] and 18.63 ± 1.82% [50 nM]; and for inhibitor = 17.32 ± 1.2 [25 nM] and 16.3 ± 1.20% [50 nM]) or let7d-5p (for mimic = 19.39 ± 2.07% [25 nM] and 19.29 ± 1.08% [50 nM]; and for inhibitor = 18.1 ± 0.91% [25 nM] and 16.86 ± 2.5% [50 nM]) transfected MEFs compared with the corresponding controls, indicating that these miRNAs exhibit no functional effect on HSV-1 replication (Figs. 3B, 3C, Supplementary Figs. S2A, S2B). Fluorescent microscopy images further validate our flow cytometry data. We observed higher number and intensity of GFP+ MEFs in miR-329-3p but not miR-184-3p and let-7d-5p overexpressing cells strongly suggests its key role in regulating the HSV-1 replication (Fig. 3D). We also performed HSV-1 replication experiments in HCEs transfected with miRNA mimic or inhibitors and obtained similar results as observed in MEFs (Supplementary Figs. S3A–S3C, S4).

Next, we evaluated expression of viral late proteins gB and VP16 in the HSV-1 infected MEFs transfected with candidate miRNA mimics and inhibitors. The expression of gB and VP16 correlates with the higher replication in miR-329 mimic expressing cells further validating our viral replication data (Fig. 3E). Overall, these assays identify miR-329 as a pro-viral miRNA and its inhibition negatively impacts viral entry and replication.

HSV-1-Responsive Host miRNAs Affect Virion Production

Having confirmed that HSV-1 responsive miRNAs impair viral entry and replication, we next investigated their impact on virion production. To evaluate this, cells were transfected with 25 nM and 50 nM concentration of miRNA mimics or inhibitors (separately), and after 6 hours post-transfection infected with HSV-1 (17-GFP) at 0.1 multiplicity of infection (MOI). The supernatants and cell lysates were collected at 24 hours post-infection for virion quantification using plaque assay. The cell lysate obtained from MEFs transfected with miR-329 demonstrated remarkably higher number of

Investigative Ophthalmology & Visual Science

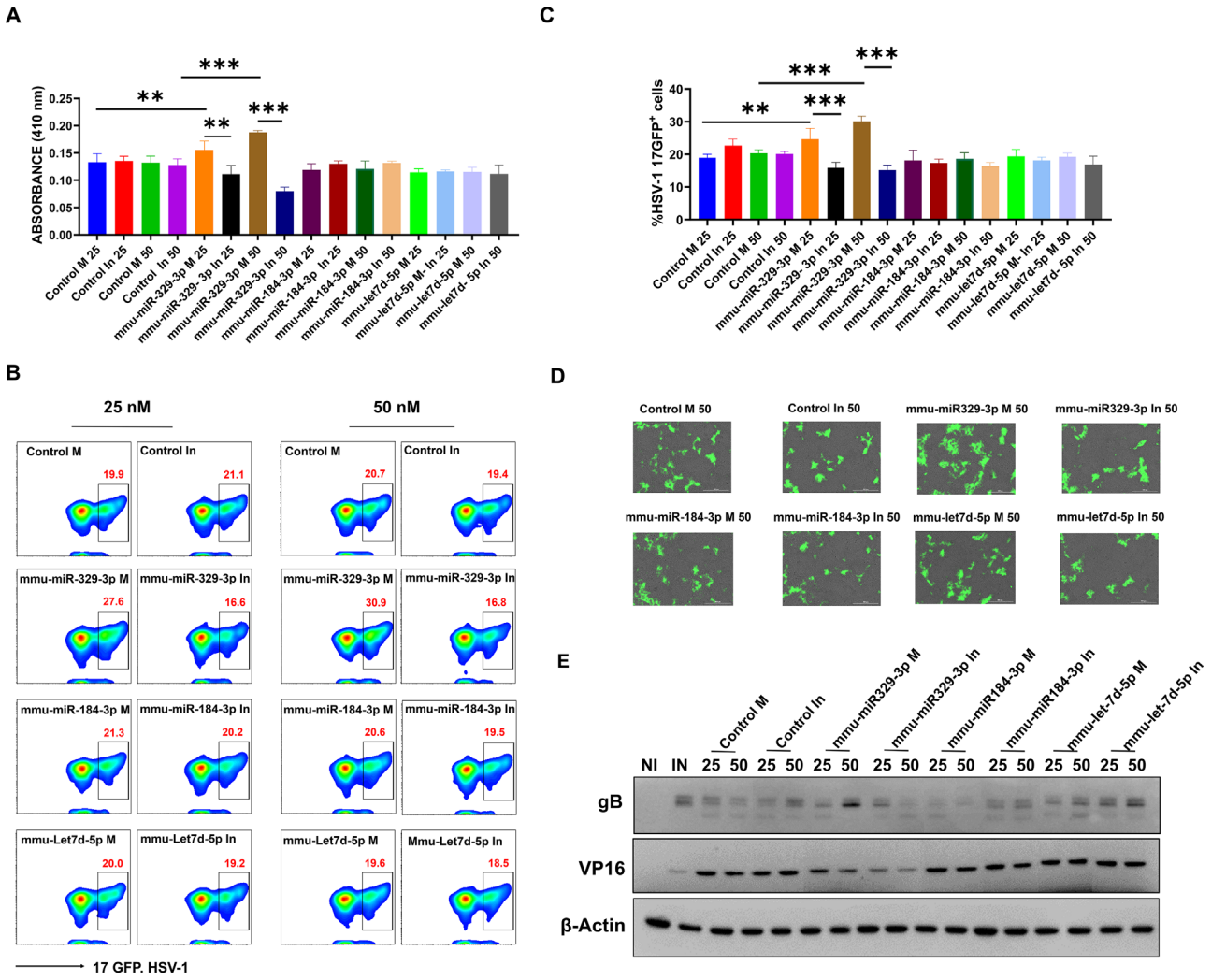

Figure 3. Host miRNAs regulate HSV-1 entry and replication in MEF cells. (**A**, **B**) Representative figure showing HSV-1 gL86 entry in MEF cells. The cells were first transfected with different concentrations (25 nM and 50 nM) of miRNA mimics inhibitors, and scrambled miRNA mimic/ inhibitors (control) and then infected with HSV-1 gL86. Viral entry was quantified 6 hours post-infection using a colorimetric assay, and absorbance was measured at 410 nm in the microplate reader. (**B**) Scatter plot depicting the GFP+ cells as infected with 17 GFP HSV-1. Total 20,000 event was acquired during flow cytometry done in cytotflex. (**C**) Overall quantitation of GFP+ cells from four replicates. (**D**) Representative overlay images of HSV-1 infected cells 24 hours post-infection. (**E**) Western blotting showing HSV-1 replication in MEFs using specific antibodies for HSV-1 proteins: VP16 and gB. More presence of these proteins reflects the replication of HSV-1. In (**B**) and (**C**) percentage of GFP+ cells were calculated in FlowJo 10.9.0. In (**A, D**) bars are generated in GraphPad 10. Data presented here: mean ± S.D.; significance assessed by 1-way ANOVA (*$P < 0.05$; **$P < 0.01$; ***$P < 0.005$; ****$P < 0.0005$). M, miRNA mimic. In, miRNA inhibitor.

plaques ($4.8 \times 10^5 \pm 2.78 \times 10^5$) compared with the controls ($8.16 \times 10^4 \pm 1.52 \times 10^4$), miR-184-3p ($1.20 \times 10^5 \pm 2.6 \times 10^4$) or let-7d-3p ($1.56 \times 10^5 \pm 6.33 \times 10^4$) mimic when the mimic were transfected at 25 nM concentration. At a higher dose of miR-329 mimic, we noticed even more significant increase in plaques correlating our previous data (Figs. 4A–C). Compared with control mimic and inhibitors ($2.83 \times 10^4 \pm 2.88 \times 10^3$ and $3.93 \times 10^4 \pm 1.50 \times 10^3$), we noticed a higher number of plaques ($2.36 \times 10^6 \pm 1.40 \times 10^5$ and $1.23 \times 10^4 \pm 2.51 \times 10^3$) in miR-329 mimic and inhibitor transfection, whereas none of the miR-184-3p mimic and inhibitor ($4.6 \times 10^4 \pm 5.07 \times 10^3$ and $1.11 \times 10^4 \pm 5.77 \times 10^2$), and let-7d mimic and inhibitor ($1.13 \times 10^4 \pm 1.60 \times 10^3$ and $7.66 \times 10^3 \pm 3.81 \times 10^3$) showed significant differences in plaque counts. HCE transfected with candidate miRNA mimics and inhibitors also showed similar patterns in plaque counts as MEFs; however, the differences were not as remarkable as observed in MEFs indicating some cell type specific affect (Supplementary Figs. S5A–D).

HSV-1-Responsive Host miRNAs Downregulate TLR9 Signaling Pathway

Our IPA results identified multiple predicted targets for miR-329 including those involved in TLR signaling and interferon pathways. We noticed TLR9, a key sensor of DNA viruses that trigger innate and adaptive immune responses by recognizing unmethylated CpG motifs in viral DNA,[34,35] as a potential gene target of mmu-miR-329-3p. To validate our bioinformatic observations, we examined if mmu-miR-329-3p regu-

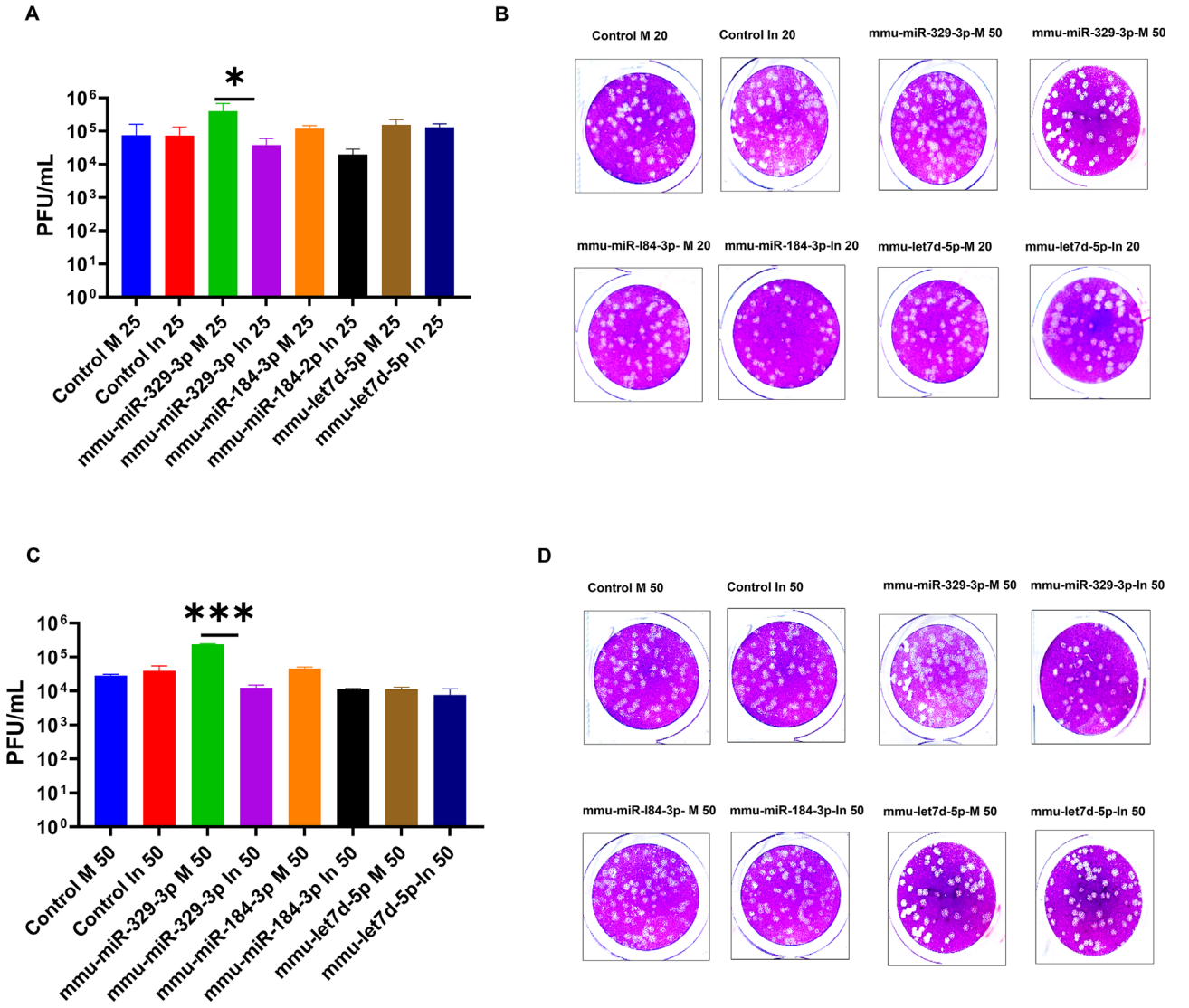

Figure 4. Assessment of viral particles from the culture supernatants of MEFs transfected with miRNAs. These cells were previously transfected with different concentrations of miRNA mimics, inhibitors, and scrambled miRNA mimic/ inhibitors (control), and were infected with HSV-1 (17-GFP) at 0.1 MOI. (**A**, **C**) Quantitation of HSV-1 titers at Assessment of viral titers in MEFs transfected with 25 nM and 50 nM concentrations of miRNAs mimics and inhibitors. (**C**, **D**) Representative figure showing the HSV-1 plaques in MEFs transfected with 25 nM and 50 nM concentrations of miRNA mimic and inhibitors. After 24 hours of infection culture, the supernatants were serially diluted to obtain a dilution of 10^{-8} in 1 mL. Approximately, 250 uL was added on the monolayer of Vero cells grown in 24 well plate, incubated for 2 hours and the cells were overlaid with 5% methylcellulose (Sigma-Aldrich) at 37°C (5% CO_2) for 72 hours until the appearance of the plaques. The plaques were then manually counted and multiplied with the appropriate dilution factor obtain the plaque-forming units per mL (PFU/mL). Data represented as: mean ± SD; significance assessed by 1-way ANOVA (*$P < 0.05$; **$P < 0.01$; ***$P < 0.005$; ****$P < 0.0005$).

late viral recognition and antiviral signaling pathways. MEF cells transfected with miR-329 or control mimic/inhibitor were infected with HSV-1 and the expression of TLR7, TLR8, and TLR9 and their downstream signaling pathways was quantified using Western blotting. Interestingly, we obtained a dose-dependent increase in TLR9 expression in miR-329 inhibitor transfected cells (1.25-fold [25 nM] and 1.71-fold [50 nM]), whereas miR-329 mimic reduced (0.77-fold [25 nM] and 0.9-fold [50 nM]) TLR9 expression (Figs. 5A, 5B). On the contrary, the expression of TLR7 and TLR8 was unaffected upon HSV-1 infection in MEFs transfected with miRNA mimic or inhibitors. TLR9 is critical for antiviral defense, particularly through the recognition of viral DNA, activating pathways that involve key molecules. REL, a component of the NF-κB family, and phosphorylated NF-κB (pNF-κB) translocate to the nucleus to induce pro-inflammatory and immune gene expression, whereas NEMO facilitates NF-κB activation via the IKK complex. Phosphorylated IRF7 (pIRF7) also translocates to the nucleus to stimulate type I interferon production, essential for antiviral responses.[36] Next, we examined the impact of TLR9 expression on its downstream signaling molecules REL, NEMO, and IRF7. In miR-329 inhibitor transfected cells, we noticed a similar pattern of increase in the expression of downstream proteins, including REL, NEMO, and IRF7 (see Figs. 5A, 5B). Densitometry analysis revealed that miR-329-3p inhibitor led to an increase pNF-κB/NF-κB ratio. We observed higher pNF-κB/NF-κB ratio of 1.84 (25 nM) and 3.31 (50 nM)

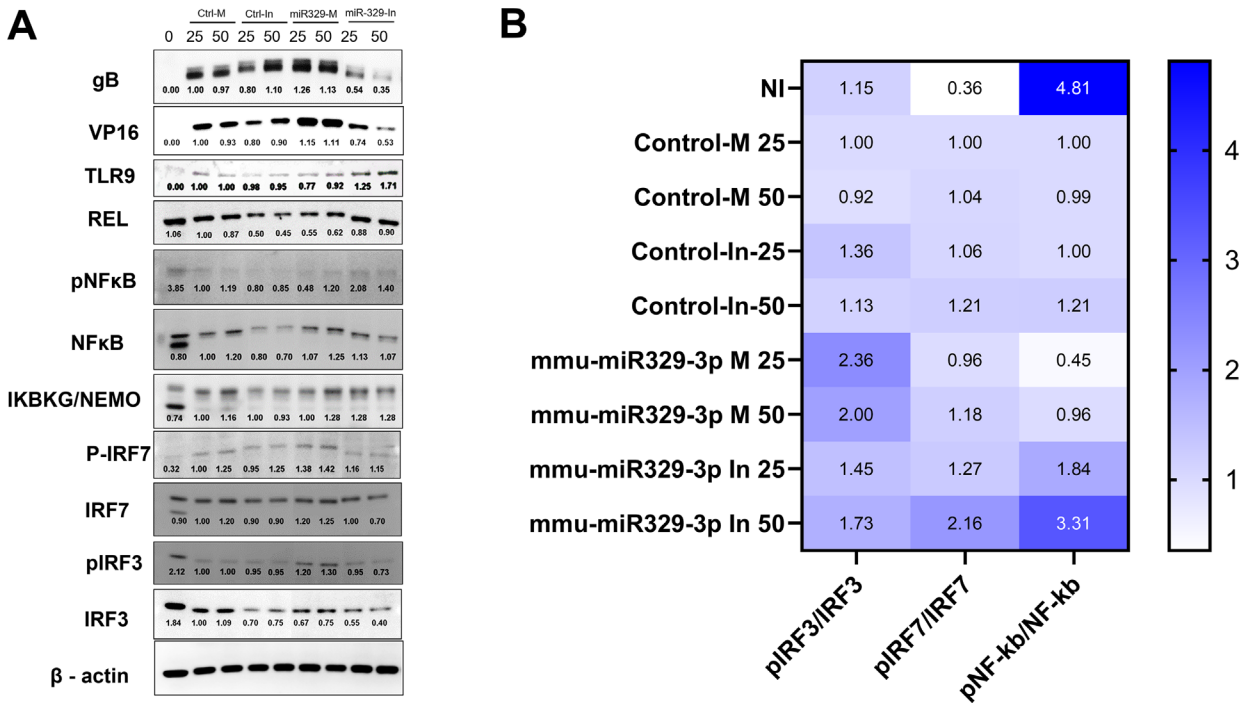

Figure 5. Host miRNA-329 dysregulate TLR-9 signaling pathway. (**A**) Representative figure demonstrating the expression of various TLR signaling pathway intermediates in miR-329 transfected and HSV-1 17 GFP infected MEF cells. MEFs cells were transfected with 25 nM and 50 nM concentrations of miRNA mimics/ inhibitors. (**B**) Quantification of phosphorylated vs total protein expression of IRF3, IRF7, and NFkB. IRF7 and NFkB are the signaling molecules of TLR-9 pathway. M, miRNA mimic; In, miRNA inhibitor. Proteins in miRNA mimic and inhibitors infected cells by Western blotting. A total 10 µg protein was loaded in each well.

in miR-329 inhibitor transfected cells compared to miR-329 mimic 0.45 (25 nM) and 0.96 (50 nM). Similarly, pIRF7/IRF7 ratios in miR-329 inhibitor transfected cells showed dose-dependent changes 1.28 and 2.16 compared to mimic 0.96 (25 nM) and 1.18 (50 nM) suggesting a robust antiviral response when miR-329 is suppressed. These findings were consistent with the reduced expression of viral proteins gB and VP16 (see Fig. 5A). Additionally, to examine the cooperation of other TLRs, we also examined the phosphorylation of IRF3, which is associated with antiviral TLR3 signaling.[37,38] Unlike the TLR9 pathway, the phosphorylation patterns of IRF3, which is associated with TLR3 and TLR4 in response to viral infections, did not follow the same trend, with a lower pIRF3/IRF3 ratio observed in the presence of the miR-329 inhibitor compared to the corresponding concentration of miR-329-3p mimic. We observed following pIRF3/IRF3 ratios miR-329-3p inhibitor versus mimic: 1.45 vs. 2.36 (25 nM) and 1.73 vs. 2.00 (50 nM; see Figs. 5A, 5B). Overall, our data suggest that downregulation of miR-329-3p is critical in activating TLR9-mediated antiviral responses during HSV-1 infection.

Discussion

HSV-1 infection poses a substantial risk to ocular health and appeared as a causative reason for herpetic keratitis (HK) and long-term visual impairment. Identifying endogenous molecules that can regulate viral infection can help develop novel targets to treat of mitigate HK and related clinical manifestation. Cellular miRNAs fine tune biological processes homeostasis by targeting cognate mRNA and may play vital antiviral functions. Interestingly, viruses have potential to change cellular miRNA repertoire during viral infection.[39–41] Various reports demonstrate that HSV-1 also takes advantage of host miRNAs (either up and downregulate) for its survival, latency, and lytic infection cycle, etc. for its endless survival in the host.[41–44] In this context, deciphering the alterations in the corneal miRNA repertoire during HSV-1 infection and its correlation with HSV-1 entry, replication and immune evasion in the cornea would be a crucial avenue of research toward improved diagnostic and therapeutic outcome in HK.

Contemplating it, we have evaluated the kinetics of cellular corneal miRNA expression in HSV-1 infected mice. Our RNA-seq data unequivocally suggests the ability of HSV-1 in reshaping corneal miRNA repertoire throughout the course of infection (day 2 to day 10 post-infection). Importantly, each time point also identifies a common and unique subset of miRNAs suggesting a key role of endogenous regulatory RNAs in shaping host-virus interaction. Changes in corneal miRNAs in microbial infection are reported but not in the context of HSV-1 infection. Boomiraj et al. reported a notable alteration in the expression profile of 75 miRNAs (fold change >2) and a probability score exceeding 0.9 in human corneas afflicted with fungal keratitis.[45] Similarly, Mun et al. (2013) also reported a significant alteration in the miRNA profile of HCE cells in response to the bacterial ocular pathogen *Pseudomonas aeruginosa*.[46] The data from this study will serve as a valuable resource to assess cellular miRNAs perturbed in HSV-1 infection and provide candidate host miRNAs involved in the onset and persistence of infection.

In particular, we noted that progressive downregulation of miR-329-3p during HSV-1 infection in the cornea. Interestingly, no report so far implicates the involvement of miR-329 in HSV-1-associated corneal infections. However, few reports show that miR-329 dysregulation in eye-related abnormalities and anti-cancer function suggesting its role in disease pathobiology. Tanaka et al. observed miR-329-3p among one of the upregulated miRNA in patients with lens-induced myopia; however, its expression was absent in the murine model of lens-induced myopia.[47] Liu et al. showed that, in colorectal cancer cells, long non-coding RNA KCNQ1OT1 upregulates its target catenin delta-1 (CTNND1) by sponging miR-329-3p and induces the proliferation, migration, and invasion, and in tandem reduces the apoptosis of colorectal cancer cells.[48] Not surprisingly, miR-329 is well studied in the context of cancer biology and is considered a tumor suppressor by inhibiting tumor growth, proliferation, and metastasis by targeting oncogenes or genes involved in cell proliferation and survival. For instance, miR-329 regulates E2F1 and CDK6 expression to control cell cycle progression.[49] Additionally, by targeting pro-angiogenic factors, such as vascular endothelial growth factor (VEGF), miR-329 is shown to regulate angiogenesis expression of miR-329, in general, is downregulated in various cancers.[50–53] Consistent with this, we also noticed a significant reduction in miR-329 during HSV-1 infection. This study, for the first time, implicates the role of miR-329 in HSV-1 induced corneal pathogenesis.

We investigated whether antiviral pathways targeting HSV-1 induced differentially expressed cornea miRNA affect the viral entry and replication. The overexpression of miR-329, but not miR-184-3p and let7d-5p, in both MEFs and HCEs resulted in a marked enhancement of HSV-1 viral entry and replication in a dose-dependent manner, whereas its inhibition exerts antagonistic outcomes. Various reports indicate that miRNAs can indeed regulate viral infections by influencing viral entry into host cells. For instance, miR-182 transcriptionally inhibit CLDN-1, which is the entry receptor for HCV.[54] Successful treatment with miR-194 mimics in various HCV-infected cell lines significantly reduces the HCV entry in Huh 7 cells via targeting its entry receptor CD81.[55] Similarly, cellular miRNAs also have the potential to effect viral replication by targeting various host factors. The miR-122 is known to promote the replication of HCV by stabilizing its genome,[56] whereas miR-142-5p has been reported to create a pro-viral milieu by targeting the non-canonical transforming growth factor beta (TGF-β) signaling pathway in Rotavirus infection.[57] To further confirm the production of active HSV-1 particles, we performed plaque assay. This observation also corroborated the prominent involvement of miR-329-3p overexpression in forming more HSV-1 plaque.

The cellular surveillance network that recognizes HSV-1 comprised of pathogen recognition receptors (PRR) viz, the TLRs, cytosolic DNA sensors, and retinoic acid-inducible gene I (RIG-I) like receptors. Besides antigen presenting cells (APC), TLRs expression is also reported in HSV-1 targeted epithelial cells in oral, ocular, genital mucosa,[58] and also in central nervous system (CNS) cells.[59,60] In epithelial cells, HSV-1 engagement with the PPRs induces type I interferons (IFNα and IFNβ), which then bind to their cognate receptors on both infected and uninfected neighboring cells to control HSV-1 infection.[61–63] Importantly, TLR3 and TLR9 are imperative in recognizing HSV-1, however, TLR2 recognizes HSV-1 proteins (e.g. gB).[64] How endogenous miRNAs participate in HSV-1 recognition and antiviral immunity is poorly understood. Our IPA analysis showed that miR-329, miR-184, and let7d-5p targets the TLR recognition and antiviral IFN pathways. All these dysregulated miRNAs were demonstrated to target various downstream proteins for these pathways, thereby suggesting their pivotal role in fine-tuning the immune response elicited against HSV-1. Importantly, our data finally demonstrate that miR-329 acts as a pro-viral factor by selectively downregulating TLR9 expression but not the other studied TLRs viz. (TLR7 and TLR8) thereby suppressing antiviral signaling molecules. We propose that miR-329 directly regulates TLR9 through its direct interaction with the 3'UTR. On the contrary, inhibition of miR-329 significantly upregulated TLR9 and its downstream effectors, including REL, NEMO, and phosphorylation of IRF7, enhancing the antiviral response. Notably, this regulatory effect was specific to the TLR9 pathway, as IRF3 phosphorylation, typically associated with TLR3/TLR4 signaling, remained unaffected by miR-329 inhibition. Together, these findings show a novel mechanism whereby miR-329 downregulation relieves a key PRR, TLR9, to potentiate antiviral immunity.

Ocular HSV-1 infection in the cornea begins with viral entry into resident cells through a multistep process, leading to a chronic immune-inflammatory response that results in corneal scarring, thinning, and neovascularization. These herpetic lesions, along with associated immune responses and neovascularization, contribute to corneal damage, leading to a chronic immuno-inflammatory disease known as herpetic stromal keratitis (HSK), which is a major cause of vision loss.[65] The miRNAs are well-known regulators of inflammation, playing roles in initiation, expansion, and resolution through both positive and negative feedback mechanisms.[66] Our study showed that HSV-1 infection perturbs immunomodulatory miRNAs suggesting an interplay between viral pathogenesis and host immune response. Using IPA analysis, we identified key miRNA players, particularly mmu-miR-184-3p and mmu-let-7d-5p (upregulated) alongside mmu-miR-329-3p and mmu-miR-2478 (downregulated), in orchestrating the host immune response by targeting multiple components within the TLR and interferon signaling pathways. Of particular significance is the downregulation of miR-329, which targets essential immune regulators like IRAK4, MYD88, and TLR9, suggesting an miRNA-mediated coordinated approach to immune modulation during viral infection.

The regulation of miRNAs largely depends on their ability to modulate NF-κB signaling, although other mechanisms have also been identified. In the current study, we observed that inhibition of miR-329 led to an increased pNF-κB/NF-κB ratio, indicative of NF-κB activation and heightened inflammation. Previous reports have highlighted the anti-inflammatory phenotype of miR-329. For instance, Song and Yang (2021) demonstrated that miR-329-3p alleviates high glucose-induced endothelial cell injury by inhibiting the TLR4/TRAF6/NF-κB signaling pathway.[67] Similarly, Garg et al. (2013) showed that miR-329 plays a critical role in mediating trophoblast apoptosis and suppressing IL-6 mRNA expression by targeting the NF-κB subunit p65.[68]

In our study, we observed a significant reduction in miR-329 expression before the onset of the inflammatory phase of HSV-1 infection. This reduction during active viral replication at the corneal surface underscores its importance in the viral life cycle. While the anti-inflammatory role of miR-329 during HSV-1 infection cannot be dismissed and warrants further investigation, our findings suggest that miR-329 predominantly plays a pro-viral role in this context.

Overall, this study provides evidence that HSV-1 responsive miR-329 manipulates the host environment for viral entry and replication in mouse cornea. We demonstrated that miR-329, a downregulated miRNA in HSV-1 infection, exhibits pro-viral function when overexpressed, whereas its inhibition reduced viral replication. Mechanistically, miR-329 targets TLR9, an endosomal DNA virus recognition molecule, and downstream antiviral signaling activation. Therefore, miR-329 is essential in mounting robust antiviral function. Further exploration of therapeutic potential of miR-329 (and potentially other miRNAs) in corneal HSV-1 infection will unveil new research avenues to combat the disease. In addition, because this study focused on male mice, we recognize that sex differences may influence the progression of HSV-1 infection and the host miRNA response. Future studies will be needed to investigate the potential impact of sex on viral pathogenesis and miRNA regulation in the context of HSV-1 ocular infection.

Acknowledgments

Supported by the National Institutes of Health grants R01 EY033622, EY024710, R01 EY029426, and P30 EY001792 (D.S.).

Disclosure: **P. Sharma**, None; **R.A. Naqvi,** None; **H. Borase**, None; **D. Kapoor**, None; **A. Valverde**, None; **K. Capistrano**, None; **T. Yadavalli**, None; **A.R. Naqvi**, None; **D. Shukla**, None

References

1. National Eye Institute (NEI), National Institutes of Health (NIH). Corneal conditions. Available at: www.nei.nih.gov/health/cornealdisease/#k.
2. Young RC, Hodge DO, Liesegang TJ, Baratz KH. Incidence, recurrence, and outcomes of herpes simplex virus eye disease in Olmsted County, Minnesota, 1976-2007: the effect of oral antiviral prophylaxis. *Arch Ophthalmol*. 2010;128(9):1178–1183.
3. Suryawanshi RK, Patil CD, Agelidis A, et al. mTORC2 confers neuroprotection and potentiates immunity during virus infection. *Nat Commun*. 2021;12(1):6020.
4. Ames J, Yadavalli T, Suryawanshi R, et al. OPTN is a host intrinsic restriction factor against neuroinvasive HSV-1 infection. *Nat Commun*. 2021;12(1):5401.
5. Hadigal SR, Agelidis AM, Karasneh GA, et al. Heparanase is a host enzyme required for herpes simplex virus-1 release from cells. *Nat Commun*. 2015;6:6985.
6. Agelidis AM, Hadigal SR, Jaishankar D, Shukla D. Viral activation of heparanase drives pathogenesis of herpes simplex virus-1. *Cell Rep*. 2017;20(2):439–450.
7. Sharma P, Kapoor D, Shukla D. Role of heparanase and syndecan-1 in HSV-1 release from infected cells. *Viruses*. 2022;14(10):2156.
8. Karasneh GA, Kapoor D, Bellamkonda N, Patil CD, Shukla D. Protease, Growth factor, and heparanase-mediated syndecan-1 shedding leads to enhanced HSV-1 egress. *Viruses*. 2021;13(9):1748.
9. Girardi E, Lopez P, Pfeffer S. On the importance of host microRNA during viral infection. *Front Genet*. 2018;9:439.
10. Jopling CL, Yi M, Lancaster AM, Lemon SM, Sarnow P. Modulation of hepatitis C virus RNA abundance by a liver-specific microRNA. *Science*. 2005;309:1577–1581.
11. Henke JI, Goergen D, Zheng J, et al. microRNA-122 stimulates translation of hepatitis C virus RNA. *EMBO J*. 2008;27:3300–3310
12. Bartel DP. Metazoan microRNAs. *Cell*. 2018;173:20–51.
13. Kawamata T, Tomari Y. Making RISC. *Trends Biochem Sci*. 2010;35:368–376.
14. Bartel DP. MicroRNAs: target recognition and regulatory functions. *Cell*. 2009;136:215–233.
15. Shimakami T, Yamane D, Jangra RK, et al. Stabilization of hepatitis C virus RNA by an Ago2-miR-122 complex. *Proc Natl Acad Sci USA*. 2012;109(3):941–946.
16. Heiss BL, Maximova OA, Thach DC, Speicher JM, Pletnev AG. MicroRNA targeting of neurotropic flavivirus: effective control of virus escape and reversion to neurovirulent phenotype. *J Virol*. 2012;86(10):5647–5659.
17. Trobaugh DW, Klimstra WB. MicroRNA regulation of RNA virus replication and pathogenesis. *Trends Mol Med*. 2017;23:80–93.
18. Marcinowski L, Tanguy M, Krmpotic A, et al. Degradation of cellular mir-27 by a novel, highly abundant viral transcript is important for efficient virus replication in vivo. *PLoS Pathog*. 2012;8:e1002510.
19. Buck AH, Perot J, Chisholm MA, et al. Post-transcriptional regulation of miR-27 in murine cytomegalovirus infection. *RNA*. 2010;16:307–315.
20. Pan D, Flores O, Umbach JL, et al. A neuron-specific host microRNA targets herpes simplex virus-1 ICP0 expression and promotes latency. *Cell Host Microbe*. 2014;15:446–456.
21. Ru J, Sun H, Fan H, et al. miR-23a facilitates the replication of HSV-1 through the suppression of interferon regulatory factor 1. *PLoS One*. 2014;9:e114021.
22. Liu X, Ru J, Zhang J, et al. miR-23a targets interferon regulatory factor 1 and modulates cellular proliferation and paclitaxel-induced apoptosis in gastric adenocarcinoma cells. *PLoS One*. 2013;8:e64707.
23. Xie Y, He S, Wang J. MicroRNA-373 facilitates HSV-1 replication through suppression of type I IFN response by targeting IRF1. *Biomed Pharmacother*. 2018;97:1409–1416.
24. Zhang Q, Guo XK, Gao L, et al. MicroRNA-23 inhibits PRRSV replication by directly targeting PRRSV RNA and possibly by upregulating type I interferons. *Virology*. 2014;450–451:182–195.
25. Choi B, Kim HA, Suh CH, Byun HO, Jung JY, Sohn S. The relevance of miRNA-21 in HSV-induced inflammation in a mouse model. *Int J Mol Sci*. 2015;16:7413–7427.
26. Liang Y, Ridzon D, Wong L, Chen C. Characterization of microRNA expression profiles in normal human tissues. *BMC Genomics*. 2007;8:166.
27. Ludwig N, Leidinger P, Becker K, et al. Distribution of miRNA expression across human tissues. *Nucleic Acids Res*. 2016;44(8):3865–3877.
28. Ratti M, Lampis A, Ghidini M, et al. MicroRNAs (miRNAs) and long non-coding RNAs (lncRNAs) as new tools for cancer therapy: first steps from bench to bedside. *Target Oncol*. 2020;15(3):261–278.
29. Gurtan AM, Sharp PA. The role of miRNAs in regulating gene expression networks. *J Mol Biol*. 2013;425(19):3582–3600.
30. Richez C, Yasuda K, Watkins AA, et al. TLR4 ligands induce IFN-alpha production by mouse conventional dendritic cells and human monocytes after IFN-beta priming. *J Immunol*. 2009;182(2):820–828.
31. Lukhele S, Boukhaled GM, Brooks DG. Type I interferon signaling, regulation and gene stimulation in chronic virus infection. *Semin Immunol*. 2019;43:101277.
32. Madavaraju K, Koganti R, Volety I, Yadavalli T, Shukla D. Herpes simplex virus cell entry mechanisms: an update. *Front Cell Infect Microbiol*. 2021;10:617578.
33. Agelidis AM, Shukla D. Cell entry mechanisms of HSV: what we have learned in recent years. *Future Virol*. 2015;10(10):1145–1154.

34. Kumagai Y, Takeuchi O, Akira S. TLR9 as a key receptor for the recognition of DNA. *Adv Drug Deliv Rev*. 2008;60(7):795–804.
35. Huang X, Yang Y. Targeting the TLR9-MyD88 pathway in the regulation of adaptive immune responses. *Expert Opin Ther Targets*. 2010;14(8):787–796.
36. Katakura K, Lee J, Rachmilewitz D, Li G, Eckmann L, Raz E. Toll-like receptor 9-induced type I IFN protects mice from experimental colitis. *J Clin Invest*. 2005;115(3):695–702.
37. Zhu J, Smith K, Hsieh PN, et al. High-throughput screening for TLR3-IFN regulatory factor 3 signaling pathway modulators identifies several antipsychotic drugs as TLR inhibitors. *J Immunol*. 2010;184(10):5768–5776.
38. Marongiu L, Gornati L, Artuso I, Zanoni I, Granucci F. Below the surface: The inner lives of TLR4 and TLR9. *J Leukoc Biol*. 2019;106(1):147–160.
39. Piedade D, Azevedo-Pereira JM. The role of microRNAs in the pathogenesis of herpesvirus infection. *Viruses*. 2016;8(6):156.
40. Naqvi AR, Shango J, Seal A, Shukla D, Nares S. Herpesviruses and microRNAs: new pathogenesis factors in oral infection and disease? *Front Immunol*. 2018;9:2099.
41. Chen S, Deng Y, Pan D. MicroRNA regulation of human herpesvirus latency. *Viruses*. 2022;14(6):1215.
42. Frappier L. Regulation of herpesvirus reactivation by host microRNAs. *J Virol*. 2015;89(5):2456–2458.
43. Deng Y, Lin Y, Chen S, et al. Neuronal miR-9 promotes HSV-1 epigenetic silencing and latency by repressing Oct-1 and Onecut family genes. *Nat Commun*. 2024;15:1991.
44. Sun B, Yang X, Hou F, et al. Regulation of host and virus genes by neuronal miR-138 favours herpes simplex virus 1 latency. *Nat Microbiol*. 2021;6:682–696.
45. Boomiraj H, Mohankumar V, Lalitha P, Devarajan B. Human corneal microRNA expression profile in fungal keratitis. *Invest Ophthalmol Vis Sci*. 2015;56(13):7939–7946.
46. Mun J, Tam C, Chan G, Kim JH, Evans D, Fleiszig S. MicroRNA-762 is upregulated in human corneal epithelial cells in response to tear fluid and Pseudomonas aeruginosa antigens and negatively regulates the expression of host defense genes encoding RNase7 and ST2. *PLoS One*. 2013;8(2):e57850.
47. Tanaka Y, Kurihara T, Hagiwara Y, et al. Ocular-component-specific miRNA expression in a murine model of lens-induced myopia. *Int J Mol Sci*. 2019;20(15):3629.
48. Liu X, Zhang Y, Wang Y, Bian C, Wang F. Long non-coding RNA KCNQ1OT1 up-regulates CTNND1 by sponging miR-329-3p to induce the proliferation, migration, invasion, and inhibit apoptosis of colorectal cancer cells. *Cancer Cell Int*. 2020;20:340.
49. Xiao B, Tan L, He B, Liu Z, Xu R. MiRNA-329 targeting E2F1 inhibits cell proliferation in glioma cells. *J Transl Med*. 2013;11:172.
50. Wang P, Luo Y, Duan H, et al. MicroRNA 329 suppresses angiogenesis by targeting CD146. *Mol Cell Biol*. 2013;33(18):3689–3699.
51. Li P, Dong J, Zhou X, et al. Expression patterns of microRNA-329 and its clinical performance in diagnosis and prognosis of breast cancer. *Onco Targets Ther*. 2017;10:5711–5718.
52. Wang X, Lu X, Zhang T, et al. mir-329 restricts tumor growth by targeting grb2 in pancreatic cancer. *Oncotarget*. 2016;7(16):21441–21453.
53. Wu L, Pei F, Men X, Wang K, Ma D. miR-329 inhibits papillary thyroid cancer progression via direct targeting WNT1. *Oncol Lett*. 2018;16(3):3561–3568.
54. Riad SE, Elhelw DS, Shawer H, et al. Disruption of claudin-1 expression by miRNA-182 alters the susceptibility to viral infectivity in HCV cell models. *Front Genet*. 2018;9:93.
55. Mekky RY, El-Ekiaby NM, Hamza MT, et al. Mir-194 is a hepatocyte gate keeper hindering HCV entry through targeting CD81 receptor. *J Infect*. 2015;70(1):78–87.
56. Joshi N, Chandane Tak M, Mukherjee A. The involvement of microRNAs in HCV and HIV infection. *Ther Adv Vaccines Immunother*. 2022;10:25151355221106104.
57. Chanda S, Nandi S, Chawla-Sarkar M. Rotavirus-induced miR-142-5p elicits proviral milieu by targeting non-canonical transforming growth factor beta signalling and apoptosis in cells. *Cell Microbiol*. 2016;18(5):733–747.
58. Herbst-Kralovetz M, Pyles R. Toll-like receptors, innate immunity and HSV pathogenesis. *Herpes*. 2006;13(2):37–41.
59. Konat GW, Kielian T, Marriott I. The role of Toll-like receptors in CNS response to microbial challenge. *J Neurochem*. 2006;99(1):1–12.
60. Aravalli RN, Peterson PK, Lokensgard JR. Toll-like receptors in defense and damage of the central nervous system. *J Neuroimmune Pharmacol*. 2007;2(4):297–312.
61. Paludan SR, Bowie AG, Horan KA, Fitzgerald KA. Recognition of herpesviruses by the innate immune system. *Nat Rev Immunol*. 2011;11:143–154.
62. Kurt-Jones EA, Orzalli MH, Knipe DM. Innate immune mechanisms and herpes simplex virus infection and disease. *Adv Anat Embryol Cell Biol*. 2017;223:49–75.
63. Pérez de Diego R, Sancho-Shimizu V, Lorenzo L, et al. Human TRAF3 adaptor molecule deficiency leads to impaired Toll-like receptor 3 response and susceptibility to herpes simplex encephalitis. *Immunity*. 2010;33(3):400–411.
64. Aravalli RN, Hu S, Rowen TN, Palmquist JM, Lokensgard JR. Cutting edge: Tlr2–mediated proinflammatory cytokine and chemokine production by microglial cells in response to herpes simplex virus. *J Immunol*. 2005;175:4189–4193.
65. Koujah L, Suryawanshi RK, Shukla D. Pathological processes activated by herpes simplex virus-1 (HSV-1) infection in the cornea. *Cell Mol Life Sci*. 2019;76:405–419.
66. Das K, Rao LV. The role of microRNAs in inflammation. *Int J Mol Sci*. 2022;23(24):15479.
67. Song G, Li L, Yang Y. MicroRNA3293p alleviates high glucose induced endothelial cell injury via inhibition of the TLR4/TRAF6/NFκB signaling pathway. *Exp Ther Med*. 2021;21(1):29.
68. Garg M, Potter JA, Abrahams VM. Identification of microRNAs that regulate TLR2-mediated trophoblast apoptosis and inhibition of IL-6 mRNA. *PLoS One*. 2013;8(10):e77249.

Investigative Ophthalmology & Visual Science